

SCIENTIFIC REPORTS



OPEN

Flexible Sensory Platform Based on Oxide-based Neuromorphic Transistors

Ning Liu^{1,2}, Li Qiang Zhu², Ping Feng¹, Chang Jin Wan², Yang Hui Liu², Yi Shi¹ & Qing Wan^{1,2}

Received: 22 June 2015
Accepted: 09 November 2015
Published: 11 December 2015

Inspired by the dendritic integration and spiking operation of a biological neuron, flexible oxide-based neuromorphic transistors with multiple input gates are fabricated on flexible plastic substrates for pH sensor applications. When such device is operated in a quasi-static dual-gate synergic sensing mode, it shows a high pH sensitivity of ~ 105 mV/pH. Our results also demonstrate that single-spike dynamic mode can remarkably improve pH sensitivity and reduce response/recover time and power consumption. Moreover, we find that an appropriate negative bias applied on the sensing gate electrode can further enhance the pH sensitivity and reduce the power consumption. Our flexible neuromorphic transistors provide a new-concept sensory platform for biochemical detection with high sensitivity, rapid response and ultralow power consumption.

With the recent interest in brain/computer interfaces¹, soft robotics², wearable electronics³ and skin-like sensory systems⁴, flexible devices have attracted growing attention. These emerging devices require new fabrication schemes that enable integration with soft, curvilinear and time-dynamic human tissues. Among these devices, flexible sensors are becoming increasingly significant in a wide-variety of novel applications such as *in vivo* monitoring⁵, delivery of advanced therapies⁶, artificial sense organs⁷, etc. As a fundamental component for sensor application, field-effect transistors (FETs) based sensors have been intensively investigated due to their inherent advantages of miniaturization, facilitated integration, direct transduction and label-free detection^{8–11}. The classical sensing mechanism of the FET-based sensor is attributed to a charge-dependent interfacial potential due to the adsorption of potential-determining species at sensing membrane/electrolyte interface¹². The sensitivity is limited to ~ 59.2 mV/decade (Nernst limit) at room temperature when the threshold voltage (V_{th}) is recorded as the output signal. It should be noted here that above mentioned measurements are based on the quasi-static electrostatic coupling mode, which potentially increases the time consumption and energy dissipation. But in smart sensory platforms, such as implantable devices and wearable sensory systems, low power consumption is one of the most important pre-requisites.

Synergic integration of presynaptic inputs from the dendrites plays an important role for sensory information process and cognitive computation, and the idea of building bio-inspired solid-state devices has been around for decades^{13,14}. In 1992, Shibata *et al.* proposed Si-based neuron transistors with multiple input gates that are capacitively coupled to a floating gate¹⁵. The “on” or “off” state of the neuron transistors depends on the integrated effect of the multiple input gates. One of the unique features of the neuron transistors is the ultralow power dissipation during calculation due to the gate-level sum operation in a voltage mode. From then on, Si-based neuron transistors have attracted much attention for chemical and biological detection due to the easy adjustment of threshold voltage^{16–20}. When an asymmetric gate capacitor structure is adopted, magnification of V_{th} shift can be observed in the neuron transistor when the sensing gate experiences a load from electrolyte. This device concept scales up the surface potential shift by the capacitance ratio between the sensing gate and the control gate^{21–23}. But, up to now, flexible electrolyte-gated neuron transistors with amorphous oxide channel layers for biochemical sensing applications have not been reported.

Amorphous oxide-based transistors were proposed as promising fundamental unit in sensory platform due to their low process temperature, superior electrical properties, high reliability and easy reproducibility^{24–26}. To date, remarkable sensing performances have been demonstrated in these oxide-based transistors^{27–29}. For portable applications, low-voltage operation is preferred. Electrolyte gated electric-double-layer (EDL) transistors can act

¹School of Electronic Science & Engineering, Nanjing University, Nanjing 210093, People's Republic of China. ²Ningbo Institute of Materials Technology and Engineering, Chinese Academy of Sciences, Ningbo 315201, People's Republic of China. Correspondence and requests for materials should be addressed to Y.S. (email: yshi@nju.edu.cn) or Q.W. (email: wanqing@nju.edu.cn)

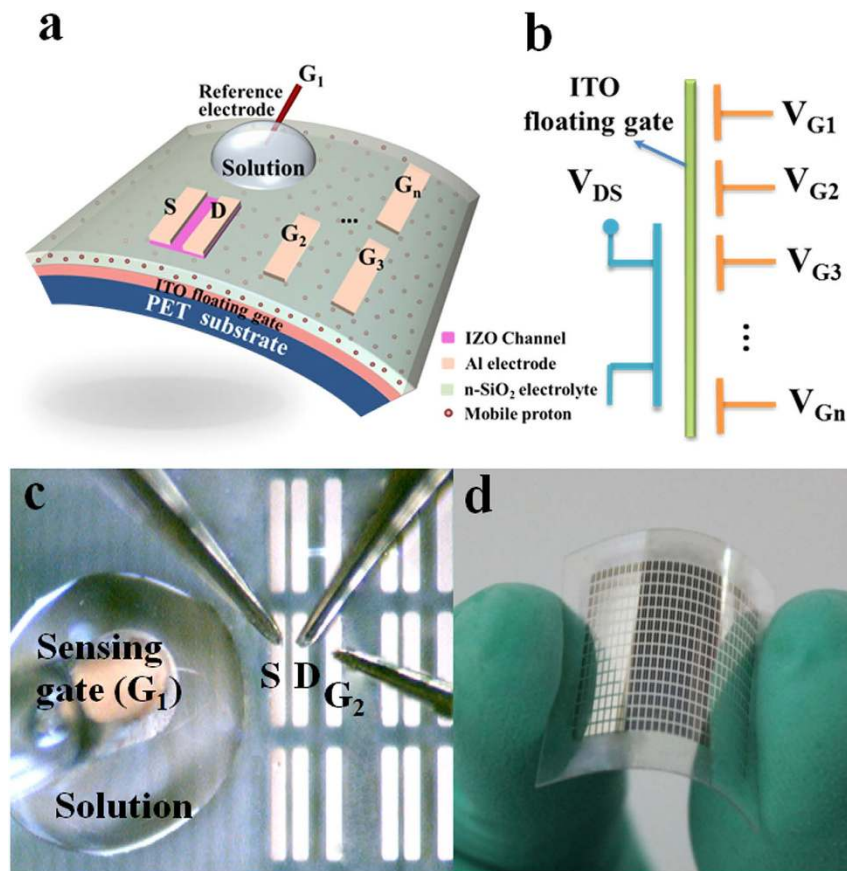


Figure 1. IZO-based neuromorphic transistor on PET substrate and its flexibility exhibition. (a) Schematic of the flexible pH sensor based on an IZO neuromorphic transistor with multiple gate electrodes. An Ag/AgCl reference electrode immersed in the solution droplet acts as the sensing gate. In-plane Al electrodes are used as the control gates. (b) The schematic image of the capacitive network of the flexible neuromorphic transistor. The carrier density of the IZO channel is modulated by the weighted sum of all inputs of sensing gate and control gates. (c) An optical microscope image of the system (Taken by Dr. Ning Liu). (d) The sensor array fabricated on a flexible PET substrate (Taken by Dr. Ning Liu).

as potential candidates with a low operation voltage due to the strong EDL modulation at the electrolyte/channel interface^{30,31}. Recently, oxide-based EDL transistors gated by solid-state inorganic electrolytes were proposed by our group^{32,33}. At the same time, artificial synapses and neuromorphic transistors with low power consumption and fundamental biological functions were mimicked in these devices^{34–36}. In the present work, flexible sensory platform based on individual protonic/electronic coupled indium-zinc-oxide (IZO) neuromorphic transistor was fabricated on plastic substrates. Such neuromorphic transistor exhibited a high sensitivity when a quasi-static dual-gate synergic modulation mode was adopted. Most importantly, single-spike dynamic sensing of such flexible neuromorphic transistor was also investigated, and pH sensing with ultra-high sensitivity, very quick response/recover time, and extremely low power consumption were realized.

Results

Figure 1a shows the schematic diagram of a flexible IZO-based neuromorphic transistor with multiple in-plane gate electrodes for pH sensing application. A miniature Ag/AgCl reference electrode immersed into a 5.0 μL pH buffer solution droplet on the nanogranular SiO_2 ($n\text{-SiO}_2$) electrolyte film acts as a sensing gate (G_1). In-plane aluminum (Al) electrodes (G_2, G_3, \dots, G_n) are used as control gates. The distinctive feature of our device is that sensing gate and all control gates are located at the same plane. The capacitive network of the neuromorphic transistor is plotted in Fig. 1b. The carrier density of the IZO channel layer can be electrostatic modulated by the weighted sum of all inputs from the sensing and control gates. The weight for each gate is directly proportional to the capacitive factor normalized by the total capacitance of the floating gate⁵. Figure 1c displays the top-view optical image of the IZO-based neuromorphic transistor sensor. The channel width (W) and length (L) is 1000 and 80 μm , respectively. As a proof of concept, only one sensing gate and one control gate electrode is used in the present work. The distance between the control gate electrode and the drain electrode is 300 μm . Figure 1d shows a picture of the IZO-based neuromorphic transistor array on PET plastic substrate, exhibiting its flexible nature under external force.

Figure 2a shows the transfer characteristics of the IZO-based EDL transistor at a constant V_{DS} of 1.5 V. Gate voltage applied on lateral Al gate electrode is swept from -1.5 V to 1.5 V and then back. A clear anticlockwise hysteresis window of ~ 0.4 V is observed, which is likely due to the mobile protons within the nanogranular SiO_2

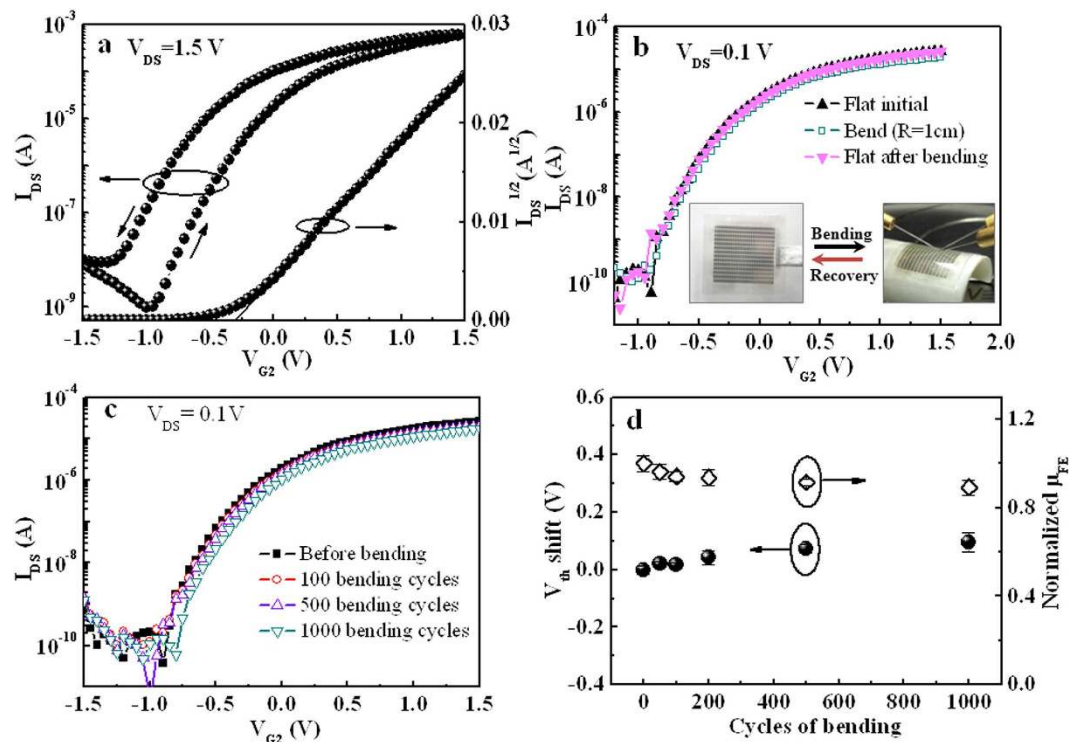


Figure 2. Electrical properties the IZO-based neuromorphic transistor and its flexibility characteristics.

(a) Transfer curves of the IZO-based neuromorphic transistor measured by sweeping the voltage on the control gate (G_2) at $V_{DS} = 1.5$ V. An anticlockwise hysteresis loop of ~ 0.4 V is observed. (b) Transfer curves of the flexible neuromorphic transistor measured before, during and after bending by a cylinder with a radius of 1.0 cm. The inset is the pictures during the measurement process (Taken by Mr.Ning Liu). (c) Transfer curves of device measured before and after repeated bending cycles by sweeping the control gate (G_2) at $V_{DS} = 0.1$ V. (d) The variations in V_{th} and μ_{FE} of the flexible neuromorphic transistor with repetitive bending cycles. Error bars represent standard deviations for 5 samples.

electrolyte³⁷. Subthreshold swings (SS), current on/off ratio (I_{on}/I_{off}) and V_{th} are estimated to be ~ 175 mV/decade, $\sim 6.4 \times 10^5$, and -0.3 V, respectively. In addition, field-effect electron mobility (μ_{FE}) at the saturation region is estimated to be ~ 12 cm²/V.s by the following equation:

$$I_{DS} = \frac{WC_i\mu_{FE}}{2L}(V_{GS} - V_{th})^2 \quad (1)$$

where C_i (~ 2.7 μ F/cm²) is the specific capacitance of the SiO₂ electrolyte measured from two in-plane Al gate electrodes at 1.0 Hz (Supporting Figure S1). For practical flexible electronics application, flexible devices should be bendable without sacrificing their electrical properties. The influence of mechanical bending on the electrical characteristics of our devices was investigated. Figure 2b shows the transfer curves recorded before, during and after bending by a cylinder with a radius of 1.0 cm. The images of the measurement process are shown in the insets of Fig. 2b. Good reproducibility is obtained on different test conditions. Moreover, mechanical stress tests have also been performed by bending the sample repeatedly. Figure 2c shows the transfer curves recorded at repetitive bending cycles. The flexible neuromorphic transistors survive after more than 1000 flex/flat cycles with negligible change in the transfer characteristics. The variations in V_{th} and μ_{FE} with the repetitive bending cycles are extracted, as shown in Fig. 2d. After 1000 cycles of bending and recovery, a small positive shift of ~ 0.1 V in V_{th} and only $\sim 10\%$ reduction in μ_{FE} are measured. The results indicate that the flexible neuromorphic transistors have good mechanical reproducibility and durability.

We will next study the pH sensing performance of the devices operated in the quasi-static mode. Figure 3a shows the transfer curves of the neuromorphic transistor based sensor operated at the linear region ($V_{DS} = 0.1$ V) with the sensing gate immersed into solution droplets with different pH values. The inset in Fig. 3a shows the layout of this normal pH sensing measurement. Clear negative shift of the transfer curve is observed when pH value decreases from 10 to 4. It has been reported that acidic solution can give rise to a more positive surface potential due to the ionic interaction at the solution/SiO₂ interface^{38,39}. In our case, positive surface potential will make protons within SiO₂ electrolyte migrate to the electrolyte/IZO channel interface, which will induce excess electrons in the IZO channel and a negative shift of transfer curve. When the gate voltage at a drain current of 10 nA is defined as the responsive voltages (V_R), a sensitivity of ~ 37.4 mV/pH is realized, as shown in Fig. 3b. This value is comparable to the reported FET sensors using SiO₂ as a sensing material⁴⁰.

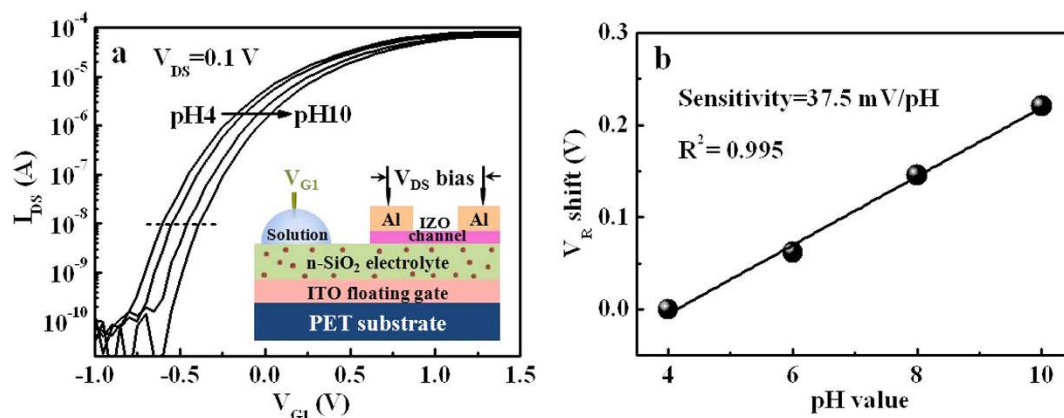


Figure 3. pH sensitivities of the IZO-based neuromorphic transistor measured in single-gate mode.

(a) Transfer curves of the neuromorphic transistor measured using the sensing gate G_1 at $V_{DS} = 0.1$ V. The pH value of the solution droplet on the sensing gate G_1 is changed from 4 to 10 at a step of 2. The inset shows the measurement schematic. (b) The sensitivity in terms of V_R shift. The data can be fitted linearly by the black line. A sensitivity of ~ 37.5 mV/pH and a linearity of ~ 0.995 are obtained.

In order to improve the sensing performance of the IZO-based neuromorphic transistor, dual-gate synergic modulation mode is investigated. During the measurements, G_1 is biased at different fixed voltages and G_2 is swept from -2.0 to 1.0 V. The measuring schematic is shown in Fig. 4a. Figure 4b shows the transfer curves ($I_{DS}-V_{G2}$) curves measured at $V_{DS} = 0.1$ V with pH value changed from 10 to 4 and V_{G1} fixed at 0.3 V and -0.6 V, respectively. Similarly, the transfer curves shift to the negative direction when the pH value decreases at a fixed V_{G1} . Here, we should point out that more obvious shifts in the transfer curve are induced by pH variation when $V_{G1} = -0.6$ V. The sensitivity in terms of V_R shift is plotted as a function of V_{G1} (Fig. 4d). The pH sensitivity increases when V_{G1} shifts from a positive value to a negative value. A maximal pH sensitivity of ~ 105 mV/pH is obtained when $V_{G1} = -0.6$ V. The improved sensitivity obtained at a negative V_{G1} is attributed to amplified capacitive coupling factor between these two gates (G_1 and G_2). Asymmetric dual-gate capacitive coupling can result in intrinsic amplification of the measured surface potential shifts. Theoretical analysis of the quasi-static pH sensing process can be found in Supporting Note 1. Jayant *et al.* also reported that this technique merely scaled the surface potential shift, but did not signify any change in the intrinsic properties of the electrolyte interface²¹. Figure 4c shows real-time responses of I_{DS} of the IZO-based neuromorphic transistor sensor in different pH solutions for 180 s at fixed $V_{DS} = 0.1$ V, $V_{G1} = 0$ V and $V_{G2} = 0.2$ V. It is observed that I_{DS} increases gradually to a stable value. The steady I_{DS} increases stepwise with discrete changes in pH value from 10 to 4. The sensitivity S of a sensor can also be defined as the relative change in channel conductance, $S = (|G - G_0|)/G_0 = \Delta G/G_0$ ⁴¹. In our case, the response conductance to pH = 10 is defined as G_0 . Therefore, the sensitivity ($\Delta G/G_0$) is estimated to be ~ 2.2 for pH = 4 at equilibrium state. We also find that the sensitivity ($\Delta G/G_0$) can be improved by a negative bias applied on sensing gate (G_1), as shown in the right axis of Fig. 4d. A highest sensitivity of ~ 38.3 is obtained at a fixed V_{G1} of -0.6 V. This value is much higher than those reported in nanoscale transistor sensors^{42,43}. This is because that an appropriate negative voltage applied on the sensing gate (G_1) can make the neuromorphic transistor operated in the subthreshold regime, in which the sensitivity in terms of current variation can be exponentially enhanced due to the most effective gating effect of charges bound on a surface⁴⁴.

Next, inspired by the spiking operation mode of a biological neuron, we have investigated the single-spike pH sensing performance of our neuromorphic transistor sensors. Due to the distinctive dynamic characteristics of the proton migration, our device presents a unique time dependent transient property. During the measurement, equilibrium is disturbed by a small voltage pulse applied on the control gate (G_2). The dynamic spike current response to such a disturbance contains the pH sensing information. After the detection, the device will quickly recover to the original equilibrium state. Moreover, during the single-spike sensing process, the energy consumption is extremely low, which is preferred for portable and wearable sensory applications. The single-spike pH sensing measurement of the detection is schematically illustrated in Fig. 5a. At first, a disturbing spike V_{G2} (0.2 V, 10 ms) was applied on control gate (G_2), and a synchronous reading spike V_D (0.02 V, 10 ms) was applied on drain electrode to measure the output current. As shown in Fig. 5b, when the pH value is changed from 4 to 10, the response current (I_{DS}) decreases from 512 to 80 nA. We also find that the logarithm of I_{DS} decreases linearly with increasing pH value, and a high sensitivity ($\Delta G/G_0$) of ~ 5.6 is estimated, as shown in Fig. 5c. The characteristic time of the dynamic process of proton migration in the nanogranular SiO_2 electrolyte is in the order of few milliseconds. The response/recover time is estimated to be ~ 5.0 milliseconds, which is much shorter than that operated in quasi-static mode. The reproducibility of the single-spike pH sensing measurement is also investigated. Figure 5d shows the response currents stimulated by repeated voltage pulse spikes with pH = 6. The results indicate a good reproducibility of single-spike detection of pH values. If we define the value of $\sigma(I_p)/\text{Ave}(I_p)$ as the noise factor, where $\sigma(I_p)$ is the standard variation of the repeated spike current peaks, and $\text{Ave}(I_p)$ is the average value of repeated spike current peaks. The value of $\sigma(I_p)/\text{Ave}(I_p)$ is calculated to be only $\sim 1.7\%$ for pH = 6. Detailed analysis of the reproducibility and noise of the spike sensing can be found in Supporting Note 2. The power consumption of our system can be

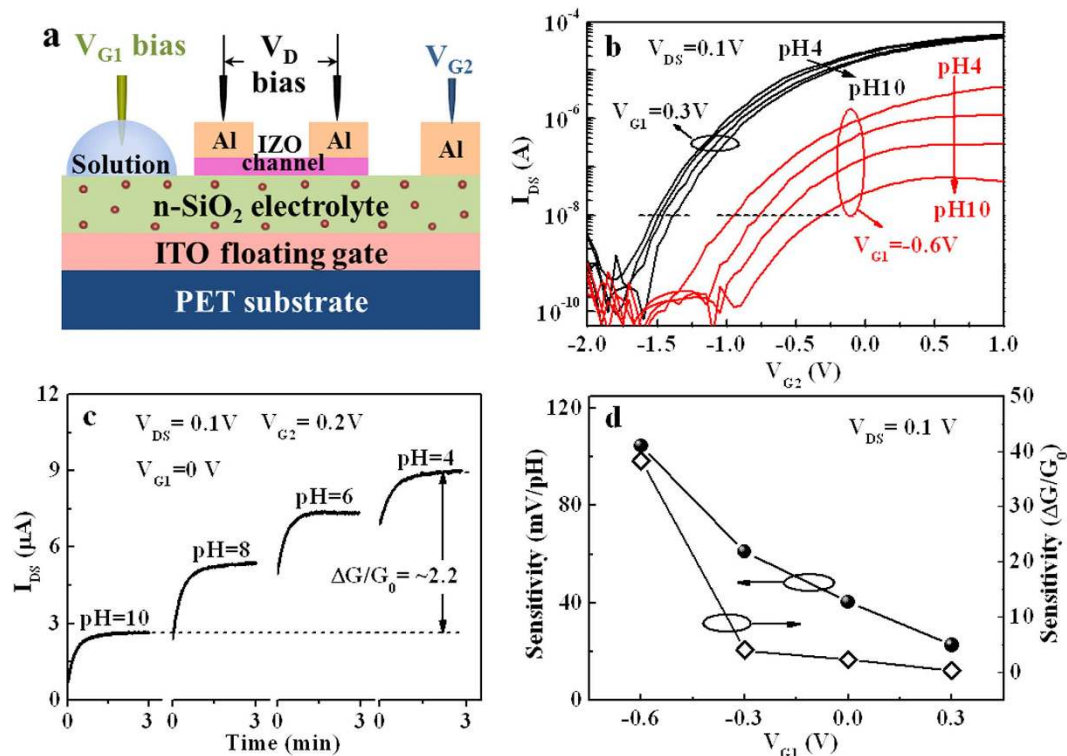


Figure 4. pH sensitivities of IZO-based neuromorphic transistor measured in dual-gate synergic modulation mode. (a) The schematic image of the measurements. (b) Transfer curves of the device measured by applying sweep voltage on the control gate (G_2) at $V_{DS} = 0.1$ V with different fixed voltages applied on G_1 . pH value of the solution droplet on G_1 increases from 4 to 10 at a step of 2. (c) The real-time responses of I_{DS} for IZO neuromorphic transistor sensors in each pH solution for 180s at $V_{DS} = 0.1$ V, $V_{G1} = 0$ V and $V_{G2} = 0.2$ V. (d) The sensitivity in terms of V_R shift and $\Delta G/G_0$ at different V_{G1} .

estimated by multiplying the reading voltage, the channel current and the spike duration time⁴⁵. Figure 5e shows the average energy dissipation for single-spike pH detection in each pH value from 10 to 4 with a spike duration time of 10 ms. The power consumption reduces from 103 pJ/spike to 15.6 pJ/spike when the pH value increases from 4 to 10. Of course, the power consumption can be further reduced by reducing the spike voltage and spike duration time. The influence of bending on the sensitivity is also investigated. As shown in Fig. 5f, after 1000 bending cycles, the sensitivity reduction is less than 10% for both quasi-static and single-spike sensing modes.

The single-spike sensing performance implemented with an asynchronous reading spike is also investigated. Figure 6a shows the sensitivity as a function of the inter-spike interval (Δt) between V_D and V_{G2} . If $\Delta t < 0$, the reading spike V_D is applied before V_{G2} . In this case, the protonic disturbance does not happen in the sensing process, thus the sensitivities are close to the equilibrium state and a sensitivity ($\Delta G/G_0$) of ~ 2.7 is obtained. When $\Delta t \geq 0$, the measured sensitivity is time interval (Δt) dependent. A highest pH sensitivity ($\Delta G/G_0$) of ~ 5.6 is obtained when $\Delta t = 0$ and it gradually reduces to 2.7 with increasing Δt . Figure 6b shows the sensitivity as a function of spike duration time. At present, in order to accurately measure a low current in the nA scale by semiconductor analyzer, the shortest spike duration we can use is 10 ms. In this case, the maximal pH sensitivity ($\Delta G/G_0$) is measured to be ~ 5.6 . We can anticipate that the sensitivity can be improved further when the spike duration time is reduced further. Detailed theoretical analysis of the influence of spike duration on the sensitivity can be found in **Supporting Note 3**. We also find that the sensitivity decreases gradually to ~ 2.4 when the spike duration increases to 2 s. These results indicate that the neuromorphic transistor sensor tends to arrive at equilibrium state with the increase of spike duration. The sensitivity of single-spike pH sensing performances of our neuromorphic transistor sensor can be improved further by additional gate synergic modulation. Figure 6c shows the influence of voltage bias applied on G_1 on the sensitivity when the device is operated in single-spike mode. The pH sensitivity increases when V_{G1} shifts from positive to negative. A maximum sensitivity ($\Delta G/G_0$) of ~ 63 can be obtained when a negative voltage of -0.2 V is applied on G_1 . We also investigated the influence of voltage bias applied on V_{G1} on the energy dissipation of single-spike sensing measurement. Our results indicate that the energy dissipation can be gradually reduced when the V_{G1} is changed from 0.2 V to -0.2 V. As shown in Fig. 6d, an ultra-low energy dissipation of ~ 0.6 pJ/spike is estimated for pH = 10 at $V_{G1} = -0.2$ V with the spike duration of 10 ms. Similar to the quasi-static synergic mode, an appropriate negative V_{G1} can make the device operate in the subthreshold regime. Thus, an enhanced sensitivity can be obtained. At the same time, negative bias can reduce the spike sensing current, which is critical for energy dissipation reduction.

The use of EDL electrolyte as gate dielectrics in flexible neuromorphic transistors can obviously reduce the operation voltage down to 2.0 V. Our results also demonstrate that spiking operation could greatly reduce the

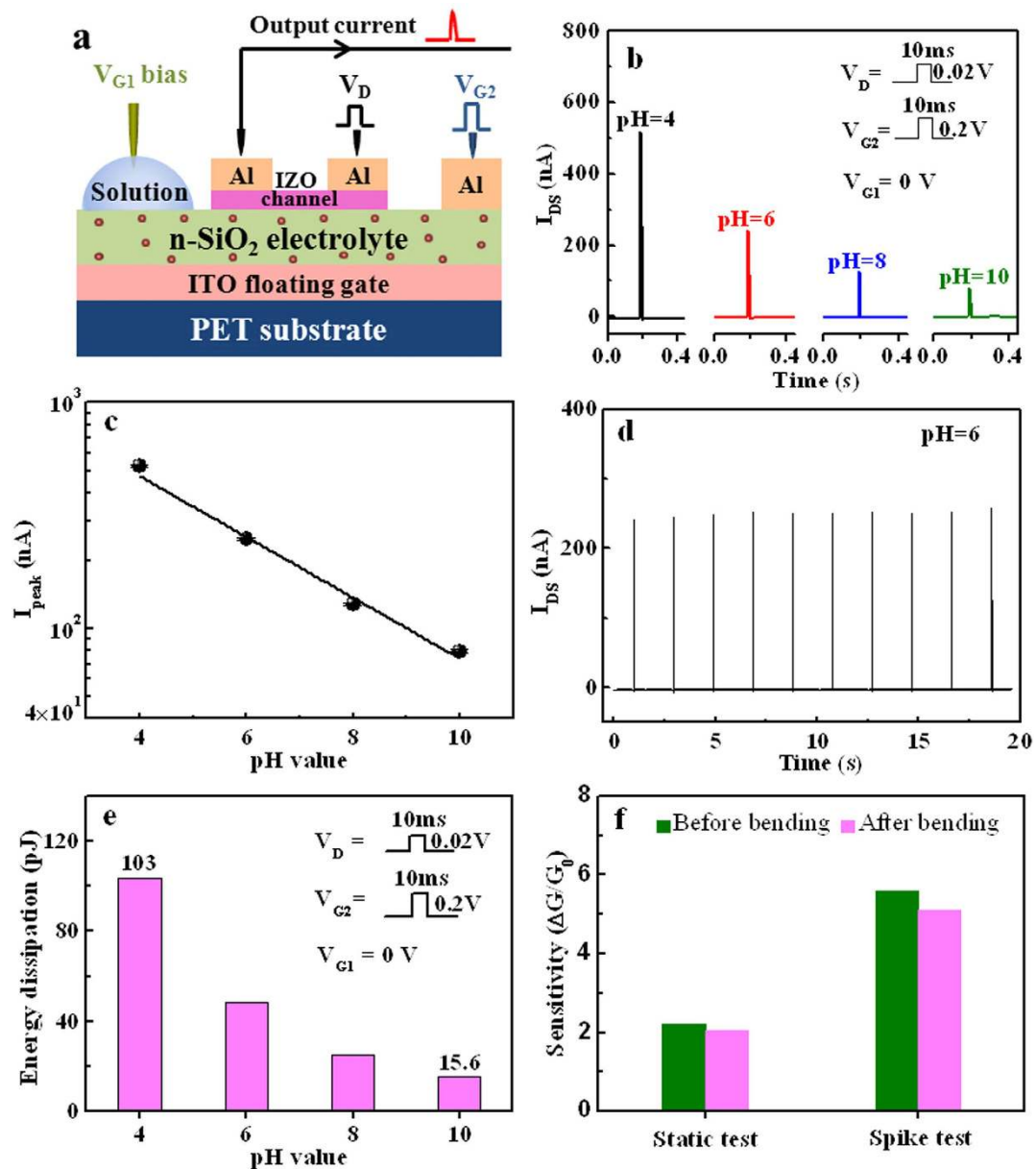


Figure 5. pH sensing performances of IZO-based neuromorphic transistor operated in a single-spike mode. (a) Schematic diagram of single-spike pH sensing measurements. (b) Single-spike measurement is performed for pH value increases from 4 to 10. The spike voltage V_{G2} (0.02 V, 10 ms) and the reading voltage V_D (0.2 V, 10 ms) are applied synchronously. The reference electrode V_{G1} is grounded. (c) The logarithm of I_{DS} peak changes linearly with the pH value of the solution. The error bars represent standard deviations for 10 samples. (d) Reproducibility of the neuromorphic transistor sensor with pH = 6. (e) pH value dependent energy dissipation operated in single-spike mode. (f) The influence of 1000 times bending on the sensitivity of the neuromorphic transistor for both quasi-static and single-spike sensing modes. Fixed biases ($V_{DS} = 0.1$ V, $V_{G1} = 0$ V, $V_{G2} = 0.2$ V) are applied in quasi-static mode. Synchronous pulse voltages V_{G2} (0.2 V, 10 ms) and V_D (0.02 V, 10 ms) with fixed V_{G1} bias of 0 V are applied in dynamic spiking mode.

power consumption because the device is usually biased at zero voltage and only low voltage spikes with very short duration time are applied. Such neuromorphic transistors are favorable for flexible and portable sensor applications. Inspired by biological neuron, our neuromorphic transistor is designed with multiple in-plane gates. At present, we only investigate the influence of the second gate on the sensing performances in both quasi-static and spiking modes. Such devices can also be proposed as multi-functional sensors, where one in-plane gate acts as modulation terminal, one in-plane gate acts as calibration terminal, and other in-plane gates act as sensing input terminals. In the future, multiple-gate stochastic resonance effects may also be explored for further sensitivity improvements and power consumption reductions when such multiple-gate devices are operated in neuromorphic sensing mode.

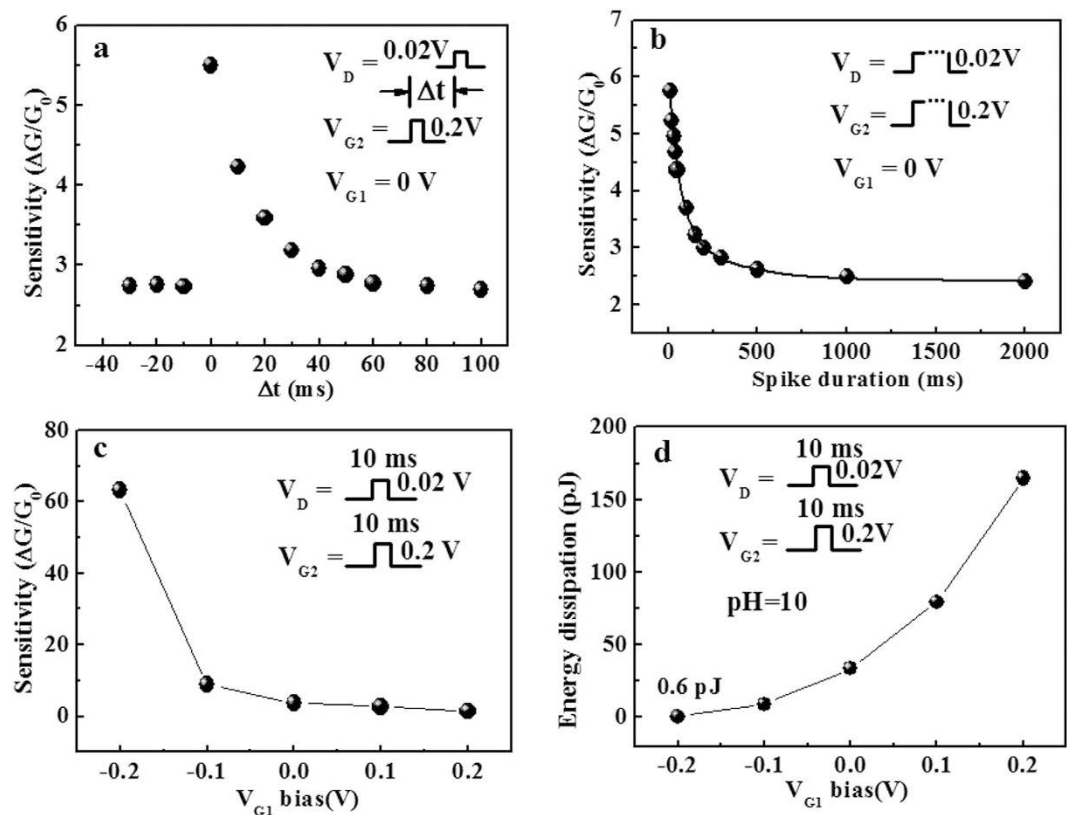


Figure 6. Influences of measuring parameters on the spike sensing performance. (a) The sensitivity as a function of the inter-spike interval between V_D and V_{G2} for asynchronous spiking sensing test. (b) The changes in sensitivity with spike duration. The solid line is the fitted curve. (c) The changes in sensitivity and energy dissipation (pH = 10) with various V_{G2} spike amplitude for synchronous spiking sensing test. (d) The changes in sensitivity and energy dissipation (pH = 10) against various V_{G1} bias.

In summary, flexible oxide-based neuromorphic transistors were fabricated on plastic substrates. A pH sensitivity of ~ 105 mV/pH was obtained for quasi-static dual-gate synergic sensing mode. Our results demonstrated that single-spike dynamic sensing mode could remarkably improve the pH sensitivity and reduce response/recover time and power consumption. We also found that appropriate depression voltage applied on the sensing gate could further enhance the pH sensitivity and reduce the power consumption. Our results provided a novel strategy for fabricating biochemical sensors with high sensitivity, rapid response and ultralow power consumption.

Methods

Fabrication of flexible oxide-based neuromorphic transistors. First, 500-nm-thick nanogranular SiO_2 electrolyte films were deposited on ITO-coated PET substrates by plasma enhanced chemical vapor deposition (PECVD) at room temperature. SiH_4 (95% $\text{SiH}_4 + 5\% \text{PH}_3$) and pure O_2 were used as reactive gases. Then, 30-nm-thick IZO channel layer was sputtered on the SiO_2 electrolyte films by using a nickel shadow mask. The sputtering was performed at a RF power of 100 W and a working pressure of 0.5 Pa using an IZO target. The channel width and length were 1000 and 80 μm , respectively. Finally, 100-nm-thick Al source/drain electrodes and in-plane gate electrodes were deposited by thermal evaporation patterned by another shadow mask.

Preparation of pH solution. pH solutions were prepared by titrating 10 mM phosphate solution with dilute hydrochloric acid or potassium hydroxide solutions. The pH value of the solutions was monitored by a commercial pH meter. All chemicals were purchased from Sinopharm Chemical Reagent Co., Ltd. (China). Such phosphate buffered solutions were used for measurements due to their strong buffer capacity to the influence of external environment. Thus, the changes in pH signal due to relaxation of charges in oxide can be ignored.

Electrical and sensing performance characterizations. The sensing area of the device was immersed in deionized water for 24 hours before measurements. Frequency-dependent capacitances of the SiO_2 electrolyte films were characterized by a Solartron 1260A Impedance Analyzer in air ambient with a relative humidity of $\sim 55\%$. Transistor characteristics and pH sensing performance were recorded by a semiconductor parameter characterization system (Keithley 4200 SCS) at room temperature. After each pH value test, the solution droplet was removed and the sensing area was rinsed two times in deionized water.

References

- Jeong, J. W. *et al.* Materials and optimized designs for human-machine interfaces via epidermal electronics. *Adv. Mater.* **25**, 6839–6846 (2013).
- Llievshi, F., Mazzeo, A. D., Shepherd, R. E., Chen, X. & Whitesides, G. M. Soft robotics for chemists. *Angew. Chem., Int. Ed.* **50**, 1890–1895 (2011).
- Zeng, W. *et al.* Fiber-based wearable electronics: A review of materials, fabrication, devices, and applications. *Adv. Mater.* **26**, 5310–5336 (2014).
- Schwartz, G. *et al.* Flexible polymer transistors with high pressure sensitivity for application in electronic skin and health monitoring. *Nat. Commun.* **4**, 1859 (2013).
- Urban, G. *et al.* Miniaturized multienzyme biosensors integrated with pH sensors on flexible polymer carriers for *in vivo* applications. *Biosens. Bioelectron.* **7**, 733–739 (1992).
- Dewire J. & Calkins, H. State-of-the-art and emerging technologies for atrial fibrillation ablation. *Nat. Rev. Cardiol.* **7**, 129–138 (2010).
- Park, S. J. *et al.* Ultrasensitive flexible graphene based field-effect transistor (FET)-type bioelectronic nose. *Nano Lett.* **12**, 5082–5090 (2012).
- Bergveld, P. Thirty years of ISFETOLOGY - What happened in the past 30 years and what may happen in the next 30 years. *Sens. Actuators, B* **88**, 1–20 (2003).
- Joo, S. & Brown, R. B. Chemical sensors with integrated electronics. *Chem. Rev.* **108**, 638–651 (2008).
- Lai, S. *et al.* Ultralow voltage, OTFT-based sensor for label-free DNA detection. *Adv. Mater.* **25**, 103–107 (2013).
- Stern, E. *et al.* Label-free immunodetection with CMOS-compatible semiconducting nanowires. *Nature* **445**, 519–522 (2007).
- Spijkman, M. *et al.* Dual-Gate Thin-Film Transistors, Integrated Circuits and Sensors. *Adv. Mater.* **23**, 3231–3242 (2011).
- Xu, N. *et al.* Nonlinear dendritic integration of sensory and motor input during an active sensing task. *Nature* **492**, 247–251 (2012).
- Spruston, N. Pyramidal neurons: dendritic structure and synaptic integration. *Nat Rev Neurosci.* **9**, 206–221 (2008).
- Shibata, T. & Ohmi, T. A functional MOS-transistor featuring gate-level weighted sum and threshold operations. *IEEE Trans. Electron Devices* **39**, 1444–1445 (1992).
- Shen, N. Y., Liu, Z., Lee, C., Minch, B. A. & Kan, E. C. Charge-based chemical sensors: a neuromorphic approach with chemoreceptive neuron MOS (CvMOS) transistors. *IEEE Trans. Electron Devices* **50**, 2171–2178 (2003).
- Shen, N. Y., Liu, Z., Jacquot, B. C., Minch, B. A. & Kan, E. C. Integration of chemical sensing and electrowetting actuation on chemoreceptive neuron MOS (CvMOS) transistors. *Sens. Actuators, B* **102**, 35–43 (2004).
- Jacquot, B. C., Munoz, N., Branch, D. W. & Kan, E. C. Non-Faradaic electrochemical detection of protein interactions by integrated neuromorphic CMOS sensors. *Biosens. Bioelectron.* **23**, 1503–1511 (2008).
- Ingebrandt, S., Yeung, C. K., Krause, M. & Offenhausser, A. Neuron-transistor coupling: interpretation of individual extracellular recorded signals. *Eur. Biophys. J.* **34**, 144–154 (2005).
- Jacquot, B. C., Lee, C., Shen, Y. N. & Kan, E. C. Time-resolved charge transport sensing by chemoreceptive neuron MOS transistors (CvMOS) with microfluidic channels. *IEEE Sens. J.* **7**, 1429–1434 (2007).
- Jayant, K. *et al.* Programmable ion-sensitive transistor interfaces. I. Electrochemical gating. *Phys. Rev. E* **88**, 012801 (2013).
- Go, J., Nair, P. R. & Alam, M. A. Theory of signal and noise in double-gated nanoscale electronic pH sensors. *J. Appl. Phys.* **112**, 034516 (2012).
- Kaisti, M., Zhang, Q., Prabhu, A., Lehmusvuori A. & Rahman, A. An ion-sensitive floating gate FET model: operating principles and electrofluidic gating. *IEEE Transactions on Electron Devices* **62**, 2628–2635 (2015).
- Nomura, K. *et al.* Room-temperature fabrication of transparent flexible thin-film transistors using amorphous oxide semiconductors. *Nature* **432**, 488–492 (2004).
- Fortunato, E., Barquinha, P. & Martins, R. Oxide semiconductor thin-film transistors: a review of recent advances. *Adv. Mater.* **24**, 2945–2986 (2012).
- Jung, J. *et al.* Approaches to label-free flexible DNA biosensors using low-temperature solution-processed InZnO thin-film transistors. *Biosens. Bioelectron.* **55**, 99–105 (2014).
- Jang, H. J., Gu, J. G. & Cho, W. J. Sensitivity enhancement of amorphous InGaZnO thin film transistor based extended gate field-effect transistors with dual-gate operation. *Sens. Actuators B: Chem.* **181**, 880–884 (2013).
- Guo, D. *et al.* Indium-tin-oxide thin film transistor biosensors for label-free detection of avian influenza virus H5N1. *Anal. Chim. Acta.* **773**, 83–88 (2013).
- Kim, S. J. *et al.* Low-cost label-free electrical detection of artificial DNA nanostructures using solution-processed oxide thin-film transistors. *ACS Appl. Mater. Interfaces* **5**, 10715–10720 (2013).
- Buth, F., Donner, A., Sachsenhauser, M., Stutzmann, M. & Garrido, J. A. Biofunctional electrolyte-gated organic field-effect transistors. *Adv. Mater.* **24**, 4511–4517 (2012).
- White, S. P., Dorfman, K. D. & Frisbie, C. D. Label-free DNA sensing platform with low-voltage electrolyte-gated transistors. *Anal. Chem.* **87**, 1861–1866 (2015).
- Lu, A., Sun, J., Jiang, J. & Wan, Q. Microporous SiO₂ with huge electric-double-layer capacitance for low-voltage indium tin oxide thin-film transistors. *Appl. Phys. Lett.* **95**, 222905 (2009).
- Jiang, J., Wan, Q., Sun, J. & Lu, A. Ultralow-voltage transparent electric-double-layer thin-film transistors processed at room-temperature. *Appl. Phys. Lett.* **95**, 152114 (2009).
- Zhu, L. Q., Wan, C. J., Guo, L. Q., Shi, Y. & Wan, Q. Artificial synapse network on inorganic proton conductor for neuromorphic systems. *Nat. Commun.* **5**, 3158 (2014).
- Wan, C. J., Zhu, L. Q., Zhou, J. M., Shi, Y. & Wan, Q. Inorganic proton conducting electrolyte coupled oxide-based dendritic transistors for synaptic electronics. *Nanoscale* **6**, 4491–4497 (2014).
- Zhou, J., Liu, N., Zhu, L., Shi, Y. & Wan, Q. Energy-Efficient Artificial Synapses Based on Flexible IGZO Electric-Double-Layer Transistors. *IEEE Electron Device Lett.* **36**, 198–200 (2015).
- Lu, A., Sun, J., Jiang, J. & Wan, Q. Low-voltage transparent electric-double-layer ZnO-based thin-film transistors for portable transparent electronics. *Appl. Phys. Lett.* **96**, 043114 (2010).
- Fung, C. D., Cheung, P. W. & Ko, W. H. A generalized theory of an electrolyte-insulator-semiconductor field-effect transistor. *IEEE Trans. Electron Devices* **ED-33**, 8–18 (1986).
- Van Hal, R. E. G., Eijkel, J. C. T. & Bergveld, P. A general model to describe the electrostatic potential at electrolyte oxide interfaces. *Adv. Colloid Interface Sci.* **69**, 31–62 (1996).
- Van Hal, R. E. G., Eijkel, J. C. T. & Bergveld, P. A novel description of ISFET sensitivity with the buffer capacity and double-layer capacitance as key parameters. *Sens. Actuators, B* **24**, 201–205 (1995).
- Nair, P. R. & Alam, M. A. Design considerations of silicon nanowire biosensors. *IEEE Trans. Electron Devices* **54**, 3400 (2007).
- Cui, Y., Wei, Q. Q., Park, H. K. & Lieber, C. M. Nanowire nanosensors for highly sensitive and selective detection of biological and chemical species. *Science* **293**, 1289–1292 (2001).
- Gao, A. *et al.* Enhanced sensing of nucleic acids with silicon nanowire field effect transistor biosensors. *Nano Lett.* **12**, 5262–5268 (2012).

44. Gao, X. P., Zheng, G. & Lieber, C. M. Subthreshold regime has the optimal sensitivity for nanowire FET biosensors. *Nano Lett.* **10**, 547–552 (2010).
45. Kim, K., Chen, C. L., Truong, Q., Shen, A. M. & Chen, Y. A carbon nanotube synapse with dynamic logic and learning. *Adv. Mater.* **25**, 1693–1698 (2013).

Acknowledgements

This work was supported in part by the National Science Foundation for Distinguished Young Scholars of China (Grant No. 61425020), and in part by the National Program on Key Basic Research Project (2012CB933004), and in part by a Project Funded by the Priority Academic Program Development of Jiangsu Higher Education Institutions, and in part by the Zhejiang Provincial Natural Science Fund (LR13F040001).

Author Contributions

The manuscript was prepared by N.L., L.Q.Z., F.P. and Q.W. Device fabrication was fabricated by N.L. and Y.H.L. Measurements were performed by N.L. and C.J.W. The project was guided by Q.W. and Y.S.

Additional Information

Supplementary information accompanies this paper at <http://www.nature.com/srep>

Competing financial interests: The authors declare no competing financial interests.

How to cite this article: Liu, N. *et al.* Flexible Sensory Platform Based on Oxide-based Neuromorphic Transistors. *Sci. Rep.* **5**, 18082; doi: 10.1038/srep18082 (2015).



This work is licensed under a Creative Commons Attribution 4.0 International License. The images or other third party material in this article are included in the article's Creative Commons license, unless indicated otherwise in the credit line; if the material is not included under the Creative Commons license, users will need to obtain permission from the license holder to reproduce the material. To view a copy of this license, visit <http://creativecommons.org/licenses/by/4.0/>